SIAM J. CONTROL OPTIM.
Vol. 56, No. 2, pp. 1081–1104

OBSERVERS FOR COMPRESSIBLE NAVIER–STOKES EQUATION*

AMIT APTE†, DIDIER AUROUX‡, AND MYTHILY RAMASWAMY§

Abstract. We consider a multidimensional model of a compressible fluid in a bounded domain. We want to estimate the density and velocity of the fluid, based on the observations for only velocity. We build an observer exploiting the symmetries of the fluid dynamics laws. Our main result is that for the linearized system with full observations of the velocity field, we can find an observer which converges to the true state of the system at any desired convergence rate for finitely many but arbitrarily large number of Fourier modes. Our one-dimensional numerical results corroborate the results for the linearized, fully observed system, and also show similar convergence for the full nonlinear system and also for the case when the velocity field is observed only over a subdomain.

Key words. data assimilation, observer, Navier–Stokes equation

AMS subject classifications. 93C20, 93C95, 93B40

DOI. 10.1137/16M1060601

1. Introduction.

Data assimilation is the problem of estimating the state of a dynamical system described by an evolution equation, typically partial differential equations (PDE), using observations, often noisy and partial, of that system. This has been widely studied in the geophysical context, e.g., meteorology, oceanography, fluid flows, etc., [5, 21, 25]. One of the approaches to this state estimation problem, and the one that we study in this paper, is the construction of appropriate observers [32, Chap. 7].

Observers are essentially a modification of the original evolution equation for the system, to incorporate the observations in a feedback term, with the aim that the solution of the observer converges to the solution of the original system being observed. Observers for finite-dimensional systems have been well studied in the literature; see, for example, [32, 37]. But in many applications such as earth sciences or engineering, the systems are modeled using PDEs that are highly nonlinear and, in many instances, chaotic. In such cases of infinite-dimensional systems governed by PDEs, there are only a few examples available in the literature, mostly for linear systems and very few for nonlinear systems [23, 31, 36, 12, 16, 17, 20, 35, 26, 6, 30].

Some of the commonly used observers are Kalman filters or Luenberger observers but the main drawback of these is that they often may break intrinsic properties of the model, e.g., symmetries and/or physical constraints such as balances in geophysical models; see, for example, [15] and references therein. For nonlinear system possessing certain symmetries, it is natural to seek a correction term which also preserves those symmetries. Such an invariance may make the correction term nonlocal but it may have other desirable properties, for example, independence from the change of coordinates. Recently, there have been attempts to construct, for a variety of systems,

*Received by the editors February 8, 2016; accepted for publication (in revised form) November 6, 2017; published electronically March 27, 2018.
http://www.siam.org/journals/sicon/56-2/M106060.html
Funding: The authors would like to thank the Indo-French Centre for Applied Mathematics (IFCAM) for financial support under the "Observers and data assimilation" project.
†International Centre for Theoretical Sciences - TIFR, IISc Campus, Bangalore-560012, India (apte@icts.res.in).
‡Université Côte d'Azur, CNRS, LJAD, France (auroux@unice.fr).
§T.I.F.R Centre for Applicable Mathematics, Post Bag No. 6503, GKVK Post Office, Bangalore-560065, India (mythily@math.tifrbng.res.in).

observers based on considerations of symmetry [9, 10, 3]. The observers we construct are motivated by these recent works, as we will see in section 2. Another motivation for observer design is the computational cost: a full Kalman filter is usually too expensive for real applications, due to the size of the gain matrices, while an observer might be much more affordable, without degrading the identification process.

The main aim of this work is to develop an observer for a class of PDE inspired by earth system applications, all of which use some approximations of Navier–Stokes equations for fluid flow. In particular, we propose an observer for the nonlinear PDE (2.1) describing the evolution of a compressible, adiabatic fluid whose velocity field is observed either fully or partially. This is justified by the fact that velocity observations for fluids have become more available in the last years. We can cite floats (e.g., Argo) for oceanography, balloons for meteorology, but also all observations generated by optical flow or particle imaging velocimetry from images (including satellite images). But as we will see, the other case in which the density is observed and not the velocity is very similar. Apart from a purely theoretical motivation, the observations of sea surface density are now available [13, and references therein] and thus the study of observers with density observations is relevant.

Our main theoretical result, Theorem 3.6, supported by extensive numerical results of the one-dimensional system (section 5), is that in the case of complete observations of the velocity, an appropriate choice of parameters leads to convergence of the observer to the true solution at any prescribed rate for an arbitrarily large but finite number of Fourier modes.

There has been some work on developing observers for Navier–Stokes-based systems. The papers [35, 20, 28] work with finite-dimensional approximations of the PDE involved whereas we work with the full PDE itself. A completely different approach based on developing observers using appropriate continuous time limits of discrete time three-dimensional variational assimilation (3D-var) or Kalman filter is developed in a series of papers [22, 24, 8] and also in [7, 2, 1, 27, 18, 4]. All these papers are in the context of incompressible flows. Here we deal with the compressible model, a coupled system for density and velocity. The linearized system consists of a hyperbolic and a parabolic PDE. This coupling of mixed types poses some difficulties in tackling the system theoretically, in particular, the full nonlinear system, unlike in the case of incompressible Navier–Stokes system. We refer to [14] and [11], where these difficulties have been overcome for the nonlinear system with highly involved techniques. In the case of the linearized system around constant steady states, we manage using Fourier series. One of the main contributions of this paper is that we also derive the decay rates for the convergence of the observers and indeed find observers that can decay arbitrarily fast. Since Navier–Stokes-based PDEs are commonly used in practical data assimilation problems in earth sciences, our work has the potential to be directly relevant to these applications, as we discuss in section 6.

The outline of the paper is as follows. The multidimensional model and the observer are both introduced in section 2. In that section, we also state the linearized version of this problem. We analyze the convergence of this proposed observer for the linearized PDE in section 3 and prove the main result Theorem 3.6. We also briefly discuss the difficulties that arise in the theoretical analysis of the nonlinear equation or of the cases with either partial observations or unknown forcing for the linearized equations. In section 5, we present one-dimensional numerical results to substantiate the linear theory. We also present the numerical results showing the efficacy of the observer in estimating the true solution for the partially observed linear system, the

observer in the case of unknown forcing term, and the fully nonlinear case. The last section, section 6, discusses some future directions of research.

2. Compressible Navier–Stokes equations and observers. In this paper, we study a model of a compressible fluid in a bounded domain. The density $\rho(t,x)$ and velocity $u(t,x)$ of the fluid form the state vector of this model and they obey the following compressible Navier–Stokes system in n-dimensions:

$$\rho_t + \nabla\cdot(\rho u) = 0\,, \quad \rho\,[u_t + (u\cdot\nabla)u] = -\nabla p(\rho) + \mu\Delta u + (\lambda+\mu)\nabla(\nabla\cdot u)\,, \tag{2.1}$$

where λ and μ are the Lamé parameters, satisfying the standard assumptions of $\mu > 0$ and $\lambda + 2\mu/3 \geq 0$ [34, 33]. The pressure p is given by the adiabatic equation of state, $p(\rho) = \rho^\gamma$ with γ, the adiabatic exponent, taken to be 1.4 for the numerical results discussed in section 5. We consider solutions over a finite time interval $[0,T]$ for the space domain $[0,1]^n \subset \mathbb{R}^n$ with periodic boundary conditions:

$$\rho(t,x) = \rho(t,x+e_k) \quad \forall\ (t,x) \in [0,T]\times[0,1]^n \quad \forall\ 1\leq k\leq n\,, \tag{2.2}$$

and similar periodic conditions for $u(t,x)$ and for all derivatives of ρ and u, where $e_k = (0,\dots,1,\dots,0)$ with the 1 in the kth place.

We assume that the initial conditions $\rho(0,x) = \rho_I(x)$ and $u(0,x) = u_I(x)$ are unknown, but we have some information on the solution $u(t,x)$ of (2.1). The goal is to build an observer $(\hat\rho,\hat u)$ for this system in such a way that both the density and the velocity of the observer $(\hat\rho,\hat u)$ converge towards the solution (ρ,u). We will assume that we have observations of the velocity denoted by $u(t,x)$ for $t\in[0,T]$ and $x\in\Omega\subset[0,1]^n$, where Ω is a subset of $[0,1]^n$. For most of the theoretical study we will consider $\Omega = [0,1]^n$ while for the numerical study of the one-dimensional problem, we will consider $\Omega = [0,L]$ with $0 < L \leq 1$.

2.1. Observers. We introduce the observer $(\hat\rho,\hat u)$, based on the symmetries for the system, satisfying the following set of equations:

$$\begin{aligned} \hat\rho_t + \nabla\cdot(\hat\rho\hat u) &= F_\rho(\hat\rho,\hat u,u)\,,\\ \hat\rho\,[\hat u_t + (\hat u\cdot\nabla)\hat u] &= -\nabla p(\hat\rho) + \mu\Delta\hat u + (\lambda+\mu)\nabla(\nabla\cdot\hat u) + F_u(\hat\rho,\hat u,u)\,. \end{aligned} \tag{2.3}$$

As there are no observations of the density, we first assume that the feedback terms do not depend on $\hat\rho$. Additionally, since these terms should be equal to 0 when u and $\hat u$ coincide, it is reasonable to consider the following classes of functions:

$$F_\rho(\hat\rho,\hat u,u) = \varphi_\rho * D_\rho(u-\hat u)\,, \quad F_u(\hat\rho,\hat u,u) = \varphi_u * D_u(u-\hat u), \tag{2.4}$$

where D_ρ and D_u are differential (or integral) operators (e.g., ∇, ∂_t, ...), and φ_ρ and φ_u are convolution kernels. We assume that these kernels are time independent and hence only functions of x, and we assume that they are isotropic. With this choice, the observer preserves the symmetries of the system, since the correction terms are based on a convolution product with an isotropic kernel, making it invariant by rotation or translation. Moreover, observations may be noisy, so the involvement of a convolution kernel leads to an observer that is inherently robust to noise.

Note that for the case of observations over partial domains, i.e., when $\Omega \neq [0,1]^n$, the feedback terms are present only in Ω so that we essentially write the feedback term as

$$F_\rho(\hat\rho,\hat u,u) = \varphi_\rho * D_\rho\left[(u-\hat u)\mathbb{1}_\Omega\right]\,, \quad F_u(\hat\rho,\hat u,u) = \varphi_u * D_u\left[(u-\hat u)\mathbb{1}_\Omega\right]\,. \tag{2.5}$$

We would like to examine the convergence of the observer solution $(\hat{\rho}, \hat{u})$ to the solution of the observed system (ρ, u) asymptotically in time. In particular, we are interested in the rate of convergence of $\|\hat{\rho} - \rho\|$ and of $\|\hat{u} - u\|$ towards zero where we will only consider the L^2 norm in this paper.

Probably the simplest observer is defined by the Luenberger observer (or asymptotic observer) as only u is observed, then the feedback term is added only in the velocity equation ($F_\rho = 0$), and the feedback term is simply $F_u(\hat{\rho}, \hat{u}, u) = k_u(u - \hat{u})$, where $k_u > 0$ is a constant. We will study more general observers, with the aim of correcting also the density equation with the velocity, and in the process increasing the rate of convergence of the observer towards the true solution.

In order to study the theoretical behavior of the observer, we first linearize the system around a steady state of the nonlinear system (2.1) and study the convergence of the observer for the linearized system. We postpone the presentation of numerical results for the nonlinear case to section 5.5.

2.2. Linearization around an equilibrium state and linear observers. We now consider an equilibrium state consisting of constant density and velocity (ρ_0, u_0), and we linearize (2.1) around this state:

$$\begin{aligned} &\rho_t + (u_0 \cdot \nabla)\rho + \rho_0 \nabla \cdot u = 0\,, \\ &\rho_0 \left[u_t + (u_0 \cdot \nabla)u\right] = \mu \Delta u + (\lambda + \mu)\nabla(\nabla \cdot u) - \gamma \rho_0^{\gamma - 1} \nabla \rho\,, \end{aligned} \tag{2.6}$$

where only terms linear in (ρ, u) appear. Of course linearizations around nonconstant density and velocity will contain additional terms such as $(u \cdot \nabla)u_0$ and we will not consider this case in this paper.

Remark 2.1. Note that in dimensions $n \geq 2$, stationary solutions of (2.1) could be spatially varying, but in the one-dimensional case $n = 1$, we have the following result.

PROPOSITION 2.2. *The only stationary solutions of one-dimensional (1D) compressible Navier–Stokes equations* (2.1) *are constants:* $\rho(t, x) = \rho_0,\ u(t, x) = u_0$.

Proof. Let us write the stationary solution as $\rho(t, x) = \rho_0(x)$ and $u(t, x) = u_0(x)$. Then the first equation of (2.1) in one dimension gives $\rho_0(x) = C/u_0(x)$ for a constant C determined by the initial conditions. The second equation of (2.1) now reads

$$\left(C^\gamma u_0^{-\gamma} + C u_0\right)_x = \nu_0 u_{0xx} \Leftrightarrow -\gamma C^\gamma u_0^{-\gamma - 1} u_{0x} + C u_{0x} = \nu_0 u_{0xx}.$$

Let us multiply this equation by u_0 and integrate over the space domain $[0, 1]$:

$$-\gamma C^\gamma \int_0^1 u_0^{-\gamma} u_{0x}\, dx + C \int_0^1 u_0 u_{0x}\, dx = \nu \int_0^1 u_{0xx} u_0\, dx.$$

The two first integrals are both equal to zero, by considering an integration by parts, as the boundary conditions are periodic. Then

$$0 = -\nu \int_0^1 (u_{0x})^2\, dx,$$

meaning that $u_{0x} \equiv 0$. ∎

We can rewrite the solution along the characteristics of the equation. The transport coefficient for both density and velocity is u_0, hence, noting that the derivatives of $\rho(t, x + u_0 t)$ are simply $\nabla \rho(t, x + u_0 t)$ and $\rho_t(t, x + u_0 t) + (u_0 \cdot \nabla)\rho(t, x + u_0 t)$, and

similarly for derivatives of $u(t, x + u_0 t)$, (2.6) at point $(t, x + u_0 t)$ is

$$\begin{aligned} \rho_t + \rho_0 \nabla \cdot u &= 0\,, \\ \rho_0 u_t &= \mu \Delta u + (\lambda + \mu) \nabla(\nabla \cdot u) - \gamma \rho_0^{\gamma - 1} \nabla \rho\,, \end{aligned} \tag{2.7}$$

which is nothing else than (2.6) with $u_0 = 0$. So we can now assume that $u_0 = 0$ without any loss of generality. Thus we will work with this linearized Navier–Stokes system with initial conditions $\rho(0, x) = \rho_I(x)$ and $u(0, x) = u_I(x)$, and periodic boundary conditions as in (2.2).

As stated above, we assume that the initial conditions $\rho_I(x)$ and $u_I(x)$ are unknown, but we have observations of the solution $u(t, x)$ of the linearized equations (2.7). Again, the goal is to build an observer $(\hat{\rho}, \hat{u})$ for this system, in such a way that the observer $(\hat{\rho}, \hat{u})$ converges towards the solution (ρ, u). We will use the same observer as introduced in (2.3)–(2.5), except that the left-hand side is now linear, just as in (2.7):

$$\begin{aligned} \hat{\rho}_t + \rho_0 \nabla \cdot \hat{u} &= \varphi_\rho * D_\rho \left[(u - \hat{u}) \mathbb{1}_\Omega \right]\,, \\ \rho_0 \hat{u}_t &= \mu \Delta \hat{u} + (\lambda + \mu) \nabla(\nabla \cdot \hat{u}) - \gamma \rho_0^{\gamma - 1} \nabla \hat{\rho} + \varphi_u * D_u \left[(u - \hat{u}) \mathbb{1}_\Omega \right] \end{aligned} \tag{2.8}$$

with periodic boundary conditions, and initial conditions different from the true initial conditions: $\hat{\rho}(0, x) = \hat{\rho}_I(x) \neq \rho_I(x)$ and $\hat{u}(0, x) = \hat{u}_I(x) \neq u_I(x)$.

We will now present the main theoretical result about this observer in the linear case, stating that we can choose the feedback terms in order to guarantee any specified rate of convergence for an arbitrarily large but finitely many number of Fourier modes. Since we are dealing with linear PDEs, we will use the Fourier series representation as our main tool.

3. Theoretical study of an observer for n-dimensional linear Navier–Stokes system. For the case of velocity observations over the full domain ($\Omega = [0, 1]^n$), subtracting the observer equations (2.8) from the state equations (2.7), we get the following equations for the errors $r = \hat{\rho} - \rho$ and $v = \hat{u} - u$:

$$\begin{aligned} r_t + \rho_0 \nabla \cdot v &= -\varphi_\rho * D_\rho v\,, \\ \rho_0 v_t &= \mu \Delta v + (\lambda + \mu) \nabla(\nabla \cdot v) - \gamma \rho_0^{\gamma - 1} \nabla r - \varphi_u * D_u v\,, \end{aligned} \tag{3.1}$$

which are exactly identical to (2.8), with (r, v) replacing $(\hat{\rho}, \hat{u})$ and with $u = 0$.

3.1. Damped wave equation formulation. We now eliminate the density in the velocity equation, in order to get an equation for the velocity alone. As we will see, this will allow us to more easily define the observers, and more particularly the differential operators D_ρ and D_u. Starting from (3.1), we take the space derivative of the density equation, and the time derivative of the velocity equations:

$$\begin{aligned} \nabla r_t + \rho_0 \nabla(\nabla \cdot v) &= -\varphi_\rho * \nabla(D_\rho v), \\ \rho_0 v_{tt} &= \mu \Delta v_t + (\lambda + \mu) \nabla(\nabla \cdot v_t) - \gamma \rho_0^{\gamma - 1} \nabla r_t - \varphi_u * D_u v_t\,. \end{aligned}$$

We replace ∇r_t in the second equation by its expression given by the first equation, and we obtain

$$\rho_0 v_{tt} = \mu \Delta v_t + (\lambda + \mu) \nabla(\nabla \cdot v_t) + \gamma \rho_0^{\gamma} \nabla(\nabla \cdot v) + \gamma \rho_0^{\gamma - 1} \varphi_\rho * \nabla(D_\rho v) - \varphi_u * D_u v_t\,. \tag{3.2}$$

Equation (3.2) is a damped wave equation, with two forcing terms coming from the observer feedbacks. In this case, the goal is to make the difference $v = \hat{u} - u$ between the observer $\hat{u}$ and the observed velocity u converge towards 0. We want to choose D_ρ and D_u which respect the symmetries of the original system, but of course the choice is not unique. Since the observations may be noisy, we also look for the operators with a minimum number of derivatives. With this in mind, we now assume that the following differential operators are used:

$$D_\rho(f) = \rho_0 \nabla \cdot f, \quad D_u(f) = \rho_0 f, \tag{3.3}$$

which means that, up to constants, we want the velocity equation to be controlled by the velocity, and the density equation by the divergence of the velocity.

Using this choice, (3.2) rewrites as follows:

$$\rho_0 v_{tt} = \mu \Delta v_t + (\lambda + \mu)\nabla(\nabla \cdot v_t) + \gamma \rho_0^\gamma \nabla(\nabla \cdot v) + \gamma \rho_0^\gamma \varphi_\rho * \nabla(\nabla \cdot v) - \rho_0 \varphi_u * v_t \tag{3.4}$$

from where we can see that the last term (with φ_u) controls the first two terms on the right while the fourth term (with φ_ρ) controls the third term.

Using (3.3), the observer error equations (3.1) now read

$$\begin{aligned} r_t + \rho_0 \nabla \cdot v &= -\rho_0 \varphi_\rho * \nabla \cdot v\,, \\ \rho_0 v_t &= \mu \Delta v + (\lambda + \mu)\nabla(\nabla \cdot v) - \gamma \rho_0^{\gamma - 1} \nabla r - \rho_0 \varphi_u * v. \end{aligned} \tag{3.5}$$

We will refer to this system as the full state observer, as it corrects both velocity and density equations.

3.2. Fourier transform. We first note that (3.5) defines the solution up to a constant. Then, if the mean value m of $r(t,x)$ is not equal to 0, the solution can at best converge towards the constant m instead of 0. Hence we assume the following.

Assumption 3.1. We suppose that the mean value of $r(t,x)$ is equal to 0, i.e., the mean values of the initial conditions of $\hat{\rho}$ and ρ are the same.

Of course, this is a strong assumption as the initial state could have bias. But it is quite often assumed, at least in the data assimilation community, that bias on observations could be removed, for instance with reanalysis methods, and that noises are zero mean. Moreover, the linear system (2.6) defines the velocity up to a constant, and the observer that we propose is consistant with this. We also note that we will be able to control the mean value of the velocity, as shown below.

As we are on the domain $[0,1]^n$ with periodic boundary conditions (see (2.2)), we can consider the following Fourier decomposition of the velocity and density:

$$v(t,x) = \sum_k a_k(t) e^{i2\pi k \cdot x}, \qquad r(t,x) = \sum_k b_k(t) e^{i2\pi k \cdot x}, \tag{3.6}$$

where $a_k(t) \in \mathbb{R}^n$ and $b_k(t) \in \mathbb{R}$ are the time dependent Fourier coefficients,

$$a_k(t) = \begin{pmatrix} a_{1k}(t) \\ \vdots \\ a_{nk}(t) \end{pmatrix} \quad \text{and} \quad k = \begin{pmatrix} k_1 \\ \vdots \\ k_n \end{pmatrix} \in \mathbb{Z}^n.$$

Note that we assume $b_0 = 0$ from Assumption 3.1. We denote by $\varphi_{\rho k}$ and φ_{uk} the Fourier coefficients of the (time independent) functions $\varphi_\rho(x)$ and $\varphi_u(x)$, respectively.

Substituting (3.6) in (3.5), we obtain the following equations for mode k: for all $1 \le i \le n$,

$$\begin{aligned}\rho_0 a'_{ik}(t) = &- \left(\mu 4\pi^2 |k|^2 + \rho_0 \varphi_{uk}\right) a_{ik}(t) \\ &- (\lambda+\mu) 4\pi^2 \left(\sum_{j=1}^n a_{jk}(t) k_j\right) k_i - \gamma \rho_0^{\gamma-1} i 2\pi b_k(t) k_i,\end{aligned} \tag{3.7}$$

where $|k|^2 = \sum_{j=1}^n k_j^2$, and

$$b'_k(t) = -\rho_0 i 2\pi (1+\varphi_{\rho k}) \sum_{j=1}^n a_{jk}(t) k_j. \tag{3.8}$$

Introducing

$$y_k(t) = \begin{pmatrix} b_k(t) \\ a_{1k}(t) \\ \vdots \\ a_{nk}(t) \end{pmatrix} \in \mathbb{R}^{n+1},$$

the system (3.7)–(3.8) rewrites as

$$y'_k(t) = M_k y_k(t), \tag{3.9}$$

where M_k is the following $(n+1)\times(n+1)$ complex matrix:

$$M_k = \begin{pmatrix} 0 & c_4(1+\varphi_{\rho k}) k^T \\ -c_3 k & -(c_1|k|^2 + \varphi_{uk}) I_n - c_2 k \otimes k \end{pmatrix}, \tag{3.10}$$

where I_n is the $n \times n$ identity matrix, 0 is the scalar zero, and

$$c_1 = \frac{\mu 4\pi^2}{\rho_0}, \quad c_2 = \frac{(\lambda+\mu)4\pi^2}{\rho_0}, \quad c_3 = \gamma \rho_0^{\gamma-2} i 2\pi, \quad c_4 = -\rho_0 i 2\pi\,. \tag{3.11}$$

Remark 3.2. Note that the Fourier analysis can also be done on the damped wave equation (3.2). Substituting (3.6) into (3.2), we obtain the following equation for mode k: for all $1 \le i \le n$,

$$\begin{aligned}\rho_0 a''_{ik}(t) = &- \left(\mu 4\pi^2 |k|^2 + \rho_0 \varphi_{uk}\right) a'_{ik}(t) - (\lambda+\mu) 4\pi^2 \left(\sum_{j=1}^n a'_{jk}(t) k_j\right) k_i \\ &- \gamma \rho_0^{\gamma} (1+\varphi_{\rho k}) 4\pi^2 \left(\sum_{j=1}^n a_{jk}(t) k_j\right) k_i.\end{aligned} \tag{3.12}$$

Let

$$z_k(t) = \begin{pmatrix} a_{1k}(t) \\ \vdots \\ a_{nk}(t) \\ a'_{1k}(t) \\ \vdots \\ a'_{nk}(t) \end{pmatrix} \in \mathbb{R}^{2n},$$

then (3.12) rewrites as $z_k'(t) = N_k z_k(t)$, where N_k is the following $2n \times 2n$ matrix:

$$N_k = \begin{pmatrix} 0_n & I_n \\ -c_5(1+\varphi_{\rho k})k \otimes k & -(c_1|k|^2 + \varphi_{uk})I_n - c_2 k \otimes k \end{pmatrix}, \tag{3.13}$$

where 0_n is the $n \times n$ zero matrix, and where we recall the values of c_1 and c_2 and introduce c_5:

$$c_1 = \frac{\mu 4\pi^2}{\rho_0}, \quad c_2 = \frac{(\lambda+\mu)4\pi^2}{\rho_0}, \quad c_5 = c_3 \times c_4 = \gamma \rho_0^{\gamma-1} 4\pi^2 . \tag{3.14}$$

3.3. Spectral analysis. We now look at the eigenvalues and eigenvectors of matrix M_k. For $k \neq 0$, let $\{k_i^\perp, 1 \leq i \leq n-1\}$ be a basis of the set of vectors orthogonal to k in $\mathbb{R}^n$.

PROPOSITION 3.3.

- *For $k \neq 0$, the eigenvalues of matrix M_k are*

$$\lambda_{dk} = -\left(c_1|k|^2 + \varphi_{uk}\right), \tag{3.15}$$

$$\lambda_{\pm k} = \frac{-\left((c_1+c_2)|k|^2 + \varphi_{uk}\right) \pm \sqrt{\left((c_1+c_2)|k|^2 + \varphi_{uk}\right)^2 - 4c_5(1+\varphi_{\rho k})|k|^2}}{2}$$

with

$$c_1 = \frac{\mu 4\pi^2}{\rho_0}, \quad c_2 = \frac{(\lambda+\mu)4\pi^2}{\rho_0}, \quad c_5 = \gamma \rho_0^{\gamma-1} 4\pi^2 . \tag{3.16}$$

λ_{dk} has a multiplicity $n-1$, and the associated eigenvectors are the following $n-1$ vectors in $\mathbb{R}^{n+1}$: $\begin{pmatrix} 0 \\ k_i^\perp \end{pmatrix}$.
λ_{+k} and λ_{-k} both have a multiplicity 1, and the associated eigenvectors are, respectively, $\begin{pmatrix} c_4(1+\varphi_{\rho k})|k|^2 \\ \lambda_{+k} k \end{pmatrix}$ and $\begin{pmatrix} c_4(1+\varphi_{\rho k})|k|^2 \\ \lambda_{-k} k \end{pmatrix}$.

- *For $k = 0$, the eigenvalues of M_0 are*

$$\lambda_{d0} = -\varphi_{u0}, \quad \lambda_{+0} = 0. \tag{3.17}$$

λ_{d0} now has multiplicity n with the associated eigenvectors: $\begin{pmatrix} 0 \\ e_i \end{pmatrix}$, $\{e_i, 1 \leq i \leq n\}$ being a basis of $\mathbb{R}^n$, and λ_{+0} has multiplicity 1 with the associated eigenvector $\begin{pmatrix} 1 \\ 0_{\mathbb{R}^n} \end{pmatrix}$.

The proof is straightforward and simply consists in multiplying these eigenvectors by M_k. Note that in the case $k = 0$, the eigenvalue λ_{+0} cannot be controlled, and the associated eigenvector corresponds to constant density solutions. So, from Assumption 3.1, the projection of $r(x,t), v(x,t)$ along this eigenvector will be zero.

For $k \neq 0$, the discriminant of the quadratic equation for the eigenvalues $\lambda_{\pm k}$ is

$$\Delta_k = \left((c_1+c_2)|k|^2 + \varphi_{uk}\right)^2 - 4c_5(1+\varphi_{\rho k})|k|^2 \tag{3.18}$$

and we use the notation $\sqrt{\Delta_k} = i\sqrt{-\Delta_k}$ if the discriminant is negative.

The eigenvectors associated with λ_{dk} correspond to nonconstant divergence-free velocity solutions, for which the equation simply consists in a diffusion equation (plus the feedback term), the diffusion coefficient being λ_{dk}. Also note that the first component of the two eigenvectors associated with $\lambda_{\pm k}$ is complex, since $c_4 = -\rho_0 i 2\pi$.

We will now relate the eigenvalues of the matrix M_k to the *decay rate* of the solutions $y_k(t)$ of (3.9).

DEFINITION 3.4. *$d_k > 0$ is a decay rate of $y_k(t)$ if there exists a constant $c > 0$ such that $\|y_k(t)\| \leq ce^{-d_k t}$ for any $t \geq 0$.*

Of course, we are usually interested in the largest decay rate. In our particular situation, the eigenvalues given by (3.15) are all negative if $\varphi_{uk} \geq 0$ and $\varphi_{\rho k} \geq 0$. In such a case, it is straightforward to see that the largest decay rate is given by

$$d_k = - \max_{\lambda \in Sp(M_k)} \{\Re(\lambda)\} \tag{3.19}$$

because there exists $c > 0$ such that $\|y_k(t)\| \leq ce^{\max\{\Re(\lambda)\}t}$. Thus, the largest decay rate can be controlled by φ_{uk} and $\varphi_{\rho k}$ as we will see in the next section.

Remark 3.5. For $k \neq 0$, the eigenvalues of matrix N_k are the following:

$$\lambda_{0k} = 0, \quad \lambda_{dk}, \quad \lambda_{\pm k}, \tag{3.20}$$

where λ_{dk} and $\lambda_{\pm k}$ are given by (3.15).

The new eigenvalue λ_{0k} has a multiplicity $n-1$, and λ_{dk} still has a multiplicity $n-1$. The $n-1$ associated eigenvectors are $\begin{pmatrix} k_i^\perp \\ \lambda k_i^\perp \end{pmatrix}$ with $\lambda = \lambda_{0k}$ or λ_{dk}.

Note that the solutions corresponding to λ_{0k} are solutions of the damped wave equation (3.2), but not solutions of the original system (3.1).

These eigenvectors correspond to divergence-free solutions, either constant in time (for $\lambda = \lambda_{0k}$) or not (for $\lambda = \lambda_{dk}$).

Finally, λ_{+k} and λ_{-k} both have a multiplicity 1, and the eigenvectors are, respectively, $\begin{pmatrix} k \\ \lambda_{+k} k \end{pmatrix}$ and $\begin{pmatrix} k \\ \lambda_{-k} k \end{pmatrix}$.

Note that the eigenvalue λ_{0k} is artificial, and only appears because we took the time derivative of the velocity equation in order to eliminate the density. This is the only main difference between the M_k and N_k spectral analyses.

3.4. Main result. We now give the main result in this framework.

THEOREM 3.6. *We assume that Assumption* 3.1 *holds. For any $d > 0$, for any $K > 0$, one can find $\varphi_\rho(x)$ and $\varphi_u(x)$ such that the maximal decay rate of the errors $r(t,x)$ and $v(t,x)$, solutions of* (3.5)*, towards* 0 *is at least d for any Fourier mode k such that $|k| \leq K$. The following values can be chosen, with c_1, c_2, and c_5 given by* (3.16)*:*

$$\varphi_{u0} = d\,, \quad \varphi_{\rho 0} = 0\,, \tag{3.21}$$

$$\varphi_{uk} = \max\left\{0; d - c_1|k|^2; 2d - (c_1+c_2)|k|^2)\right\}\,, \quad 0 < |k| \leq K\,, \tag{3.22}$$

$$\varphi_{\rho k} = \max\left\{0; \frac{\left((c_1+c_2)|k|^2 + \varphi_{uk}\right)^2}{4c_5|k|^2} - 1\right\}\,, \quad 0 < |k| \leq K\,, \tag{3.23}$$

$$\varphi_{uk} = 0\,, \quad \varphi_{\rho k} = 0\,, \quad |k| > K\,. \tag{3.24}$$

In other words, for any specified decay rate, we can find convolution kernels φ_ρ and φ_u such that the observer $\hat{u}$ converges towards u at this specified rate up to any Fourier mode. Indeed, we can choose appropriate Fourier coefficients of these

kernels for any mode $k \in \mathbb{Z}^n$, but as we will see, their expression does not ensure the convergence of the Fourier series and we need to truncate the series.

Proof. Let $d > 0$, $K > 0$, and let k be a Fourier mode such that $0 < |k| \leq K$.

The case $k = 0$ is trivial: the only eigenvalue is $\lambda_{d0} = -\varphi_{u0}$, leading to the appropriate decay rate for the velocity if we choose (3.21). There is no correction on the density but the Fourier mode b_0 is 0 from Assumption 3.1.

We can see that if we use (3.22), then this choice ensures nonnegativity of all Fourier coefficients of the convolution kernels, and from (3.15), we see that $-\lambda_{dk}$ is at least d. For small modes, the diffusion process is not large enough to ensure the decay rate, so we need to add the feedback term. For larger modes, diffusion will be enough, and there is no need to add the feedback (but one can still add a feedback term, and the decay rate will become larger than the specified rate for such modes). Note that even if we drop the $\max\{0; .\}$ in (3.22), it still ensures that the decay rate will be at least d, but φ_{uk} may become negative for large modes, and this can lead to numerical instabilities.

Then, recalling (3.18), we set $\varphi_{\rho k}$ as in (3.23). This choice of $\varphi_{\rho k}$ ensures that $\Delta_k \leq 0$, and the decay rate corresponding to eigenvalues $\lambda_{\pm k}$ is then exactly $\frac{(c_1+c_2)|k|^2+\varphi_{uk}}{2}$, which is always larger than (or equal to) d, because of the choice of φ_{uk} in (3.22).

The $\max\{0, .\}$ in (3.23) is also optional, since even without the max, the discriminant Δ_k will be negative, but the nonnegativity of $\varphi_{\rho k}$ will avoid numerical instabilities.

For large modes, namely, $|k| > \sqrt{\frac{d}{c_1}}$ and $|k| > \sqrt{\frac{2d}{c_1+c_2}}$, $\varphi_{uk} = 0$, and then there is no issue in considering the inverse Fourier transform and defining a convolution kernel $\varphi_u(x)$ with these coefficients.

With the above choices, only finitely many Fourier modes of $\varphi_u(x)$ and $\varphi_\rho(x)$ are nonzero and hence the convolution kernels exist, which proves the result. ∎

Note that we could use the same definitions from (3.22)–(3.23) for larger modes ($|k| > K$), but then the Fourier series for $\varphi_\rho(x)$ does not converge, as $\varphi_{\rho k} = \mathcal{O}(|k|^2)$. So we need to truncate the series, and set $\varphi_{\rho k} = 0$ for $|k| > K$.

We also note that for large modes for which both $\varphi_{\rho k}$ and φ_{uk} are set to 0, the observer is simply a solution of the equation without any forcing term, and the largest eigenvalue is λ_{+k} (both λ_{dk} and $\lambda_{-k} \to -\infty$ when $|k| \to +\infty$). From (3.15), the decay rate is then equal to $\frac{c_5}{c_1+c_2} = \frac{\gamma\rho_0^\gamma}{\lambda+2\mu}$ asymptotically for $|k| \to +\infty$.

3.5. Observers with density observations. We have only considered observations of the velocity field so far in this paper. In this subsection, we will construct the observers for the case when the density is observed instead of velocity.

Since observations of the scalar field (density) naturally gives less information than those of a vector field (velocity) in any dimension greater than one, we will see that, as expected, we will not be able to control all the modes in the observer. In particular, we will be unable to modify the convergence rates for the eigenvectors corresponding to the diffusion eigenvalues but we will be able to get arbitrarily high convergence rates for the eigenvectors corresponding to eigenvalues $\lambda_\pm$. Since the details of the calculations are very similar to those presented above, we will only present a sketch of the results.

When we have density observations $\rho(t, x)$ instead of velocity $u(t, x)$, the observer is exactly as in the observer equations (2.8) with u being replaced by ρ. Then the equations for errors $r = \hat{\rho} - \rho$ and $v = \hat{u} - u$ will be as follows. These are the same

as (3.1) with r replacing v in the feedback terms:

$$\begin{aligned} r_t + \rho_0 \nabla \cdot v &= -\psi_\rho * \bar{D}_\rho r\,, \\ \rho_0 v_t &= \mu \Delta v + (\lambda+\mu)\nabla(\nabla\cdot v) - \gamma \rho_0^{\gamma-1}\nabla r - \psi_u * \bar{D}_u r\,. \end{aligned} \tag{3.25}$$

We see that because of the symmetries of the equations, the natural choice of the differential operators $\bar{D}_\rho$ and $\bar{D}_u$ with minimal derivatives is

$$\bar{D}_\rho(f) = f \quad \text{and} \quad \bar{D}_u(f) = \gamma\rho_0^{\gamma-1}\nabla f\,. \tag{3.26}$$

Assumption 3.7. We suppose that the mean value of $v(t,x)$ is equal to 0, i.e., the mean values of the initial conditions of $\hat{u}$ and u are the same.

Again, this is a strong assumption similar to Assumption 3.1; contrary to the density mean, the velocity mean cannot be corrected from (3.25)–(3.26).

Remark 3.8. As in the case of velocity observations, we can eliminate v in order to obtain an equation for the density alone. This can help in understanding the choice of the differential operators in the feedback terms. From the first equation of (3.25), we can extract $\rho_0\nabla\cdot v = -r_t - \psi_\rho * \bar{D}_\rho r$ and then we need to take the divergence of the second equation,

$$\rho_0\nabla\cdot v_t = \mu\nabla\cdot\Delta v + (\lambda+\mu)\nabla\cdot(\nabla(\nabla\cdot v)) - \gamma\rho_0^{\gamma-1}\nabla\cdot(\nabla r) - \psi_u * \nabla\cdot(\bar{D}_u r).$$

By choosing $\bar{D}_\rho$ and $\bar{D}_u$ as in (3.26), we get the damped wave equation for $r(x,t)$,

$$\rho_0 r_{tt} = (\lambda+2\mu)\Delta r_t + \gamma\rho_0^\gamma \Delta r + (\lambda+2\mu)\psi_\rho * \Delta r + \gamma\rho_0^\gamma \psi_u * \Delta r - \rho_0 \psi_\rho * r_t\,, \tag{3.27}$$

which again shows that the choices of $\bar{D}_u$ and $\bar{D}_\rho$ are quite natural to control the terms in the above equation.

We can then see that if we are in one dimension, $n = 1$, (3.4) and (3.27) are identical with $\varphi_u = \psi_\rho$, and $\varphi_\rho = \psi_u + ((2\mu+\lambda)\psi_\rho)/(\gamma\rho_0^\gamma)$. Thus in one dimension, observations of the density and those of velocity give the same results for rates of convergence of the observer solution.

Introducing the Fourier decomposition for (r, v) exactly like in (3.6) and the vector y_k of the Fourier coefficients, we will get a system $y_k'(t) = \bar{M}_k y_k(t)$, where $\bar{M}_k$ is the following $(n+1)\times(n+1)$ complex matrix:

$$\bar{M}_k = \begin{pmatrix} -\psi_{\rho k} & c_4 k^T \\ -c_3(1+\psi_{uk})k & -c_1|k|^2 I_n - c_2 k\otimes k \end{pmatrix}. \tag{3.28}$$

We recall the values of the constants:

$$c_1 = \frac{\mu 4\pi^2}{\rho_0},\ c_2 = \frac{(\lambda+\mu)4\pi^2}{\rho_0},\ c_3 = \gamma\rho_0^{\gamma-2} i 2\pi,\ c_4 = -\rho_0 i 2\pi,\ c_5 = c_3\times c_4 = \gamma\rho_0^{\gamma-1}4\pi^2. \tag{3.29}$$

We also recall that $\{k_i^\perp, 1\le i\le n-1\}$ is a basis of the set of vectors orthogonal to k in $\mathbb{R}^n$ if $k\neq 0$. We have then the following result.

PROPOSITION 3.9.

- *For $k\neq 0$, the eigenvalues of matrix $\bar{M}_k$ are*

$$\begin{aligned} \bar{\lambda}_{dk} &= -c_1|k|^2, \\ \bar{\lambda}_{\pm k} &= \frac{-\big((c_1+c_2)|k|^2+\psi_{\rho k}\big) \pm \sqrt{\big((c_1+c_2)|k|^2-\psi_{\rho k}\big)^2 - 4c_5(1+\psi_{uk})|k|^2}}{2}. \end{aligned} \tag{3.30}$$

The eigenvalue $\bar{\lambda}_{dk}$ *has a multiplicity* $n-1$*, with eigenvectors* $\begin{pmatrix} 0 \\ k_i^\perp \end{pmatrix}$*. The eigenvalues* $\bar{\lambda}_{\pm k}$ *both have a multiplicity* 1*, with eigenvectors* $\begin{pmatrix} c_4|k|^2 \\ (\lambda_{\pm k}+\psi_{\rho k})k \end{pmatrix}$.

- *For* $k=0$*, the eigenvalues of matrix* $\bar{M}_0$ *are*

$$\bar{\lambda}_{d0}=0, \quad \bar{\lambda}_{-0}=-\psi_{\rho 0}. \tag{3.31}$$

$\bar{\lambda}_{d0}$ *now has multiplicity* n*, with associated eigenvectors:* $\begin{pmatrix} 0 \\ e_i \end{pmatrix}$*,* $\{e_i, 1\le i\le n\}$ *being a basis of* $\mathbb{R}^n$*, and* $\bar{\lambda}_{-0}$ *having multiplicity* 1*, with the associated eigenvector* $\begin{pmatrix} 1 \\ 0_{\mathbb{R}^n} \end{pmatrix}$.

The proof of this result is straightforward; one simply has to multiply these eigenvectors by $\bar{M}_k$.

Note that for $k=0$, $\bar{\lambda}_{d0}$ cannot be controlled, but the associated eigenvectors correspond to constant velocity solutions. So from Assumption 3.7, this case does not appear. But in this case, $\bar{\lambda}_{-0}$ can be controlled, and it corresponds to constant density solutions.

For $k\neq 0$, the discriminant is

$$\bar{\Delta}_k=\big((c_1+c_2)|k|^2-\psi_{\rho k}\big)^2-4c_5(1+\psi_{uk})|k|^2 \tag{3.32}$$

and we still use the notation $\sqrt{\bar{\Delta}_k}=i\sqrt{-\bar{\Delta}_k}$ if $\bar{\Delta}_k<0$.

Note that $\bar{\lambda}_{dk}$ is independent of ψ_ρ and ψ_u and thus cannot be controlled by any choice of ψ_ρ or ψ_u. Exactly in parallel with the previous case (velocity observations) and the choice presented in (3.22)–(3.23), we have the following result.

THEOREM 3.10. *We suppose that Assumption* 3.7 *holds. For any* $d>0$*, for any* $K>0$*, one can find* $\psi_\rho(x)$ *and* $\psi_u(x)$ *such that the maximal decay rate of the errors* $r(t,x)$ *and* $v(t,x)$*, solutions of* (3.25)*, towards* 0 *is at least* $\min\{d, c_1|k|^2\}$ *for any Fourier mode* k *such that* $|k|\le K$*. The following values can be chosen, with* c_1*,* c_2*, and* c_5 *given by* (3.29)*:*

$$\psi_{\rho 0}=d\,, \quad \psi_{u0}=0\,, \tag{3.33}$$

$$\psi_{\rho k}=\max\left\{0; 2d-(c_1+c_2)|k|^2)\right\}\,, \quad 0<|k|\le K\,, \tag{3.34}$$

$$\psi_{uk}=\max\left\{0; \frac{\big((c_1+c_2)|k|^2-\psi_{\rho k}\big)^2}{4c_5|k|^2}-1\right\}\,, \quad 0<|k|\le K\,, \tag{3.35}$$

$$\psi_{uk}=0\,, \quad \psi_{\rho k}=0\,, \quad |k|>K\,. \tag{3.36}$$

The $\max(.,0)$ in (3.35) is there to ensure positiveness of all Fourier coefficients of ψ_u. It could be relaxed as it is only useful for small modes (the other term grows as $|k|^2$).

Proof. The choice of ψ_{uk} ensures that $\bar{\Delta}_k\le 0$ and the real part of $\bar{\lambda}_{\pm k}$ is then $-\frac{((c_1+c_2)|k|^2+\psi\rho k)}{2}$. Then, using (3.34), the decay rate is then at least d for all k with $|k|\le K$. ∎

We note that the modes that we cannot control to have a prespecified decay rate are the incompressible ones since the eigenvector $\begin{pmatrix} 0 \\ k_i^\perp \end{pmatrix}$ satisfies $k\cdot v_k=0$, corresponding to $\nabla\cdot v=0$. This is expected since the density observations cannot give any information about the "constant density" incompressible flow.

3.6. Remarks and comparison with the nudging feedback. We now compare the result presented in the previous sections with what can be done with the standard nudging observer, for which only the observed variable is corrected. We will use $a=(c_1+c_2)|k|^2$, $b=2\sqrt{c_5}|k|$ (see (3.29)) in the discussion in the rest of this section.

Nudging with velocity observations. In this case, there is no feedback on the density: $\varphi_\rho = 0$, and the differential operator on the velocity D_u is simply the identity (or more physically $D_u(f) = \rho_0 f$ as in (3.3)). Then (3.1) becomes

$$\begin{aligned} r_t + \rho_0 \nabla \cdot v &= 0\,, \\ \rho_0 v_t &= \mu \Delta v + (\lambda + \mu)\nabla(\nabla \cdot v) - \gamma \rho_0^{\gamma-1} \nabla r - \rho_0 \varphi_u * v\,. \end{aligned} \tag{3.37}$$

Let us fix $x = \varphi_{uk}$ for this paragraph. We can write the eigenvalues $\lambda_\pm$ from (3.15) as

$$\lambda_\pm = -\frac{1}{2}\left[(a+x) \pm \sqrt{(a+x)^2 - b^2}\right].$$

From this expression, we can find optimal decay rates as follows.

- If $a \le b$, i.e, for $|k| \le \frac{2\sqrt{c_5}}{c_1+c+2}$, it is easy to see that the real part of $-\lambda_\pm$ is maximized for $x = b - a$, and for this choice the decay rate is $b/2 = \sqrt{c_5}|k|$ which is greater than the decay rate without nudging ($x = 0$) but it cannot be made arbitrarily large as in the full state observer (see Theorem 3.6).
- If $a > b$, i.e., for $|k| > \frac{2\sqrt{c_5}}{c_1+c+2}$, we again see that the real part of $-\lambda_\pm$ is maximized for $x = 0$ and this simply gives the decay rate without nudging. Again, the full state observer presented above is better then simple nudging since we can obtain arbitrarily large decay rates up to $|k| < K$ for any fixed K.

Nudging with density observations. In this case, there is no feedback term on the velocity: $\psi_u = 0$, and the differential operator on the density $\bar{D}_\rho$ is still the identity, as in (3.26). The system (3.25) now becomes

$$\begin{aligned} r_t + \rho_0 \nabla \cdot v &= -\psi_\rho * r\,, \\ \rho_0 v_t &= \mu \Delta v + (\lambda + \mu)\nabla(\nabla \cdot v) - \gamma \rho_0^{\gamma-1} \nabla r\,. \end{aligned} \tag{3.38}$$

Let us fix $x = \psi_{\rho k}$ for this paragraph. We can write the eigenvalues $\bar{\lambda}_\pm$ from (3.30) as

$$\bar{\lambda}_\pm = -\frac{1}{2}\left[(a+x) \pm \sqrt{(a-x)^2 - b^2}\right].$$

From this expression, we can find optimal decay rates by maximizing the real part of the above expression as a function of x in exactly the same manner as the discussion in the previous paragraph. In this case, it is easy to see that the real part of $-\lambda_\pm$ is maximized for $x = b + a$, and for this choice the decay rate is $\min\{a + b/2, c_1|k|^2\}$ which is greater than the decay rate without nudging ($x = 0$) but the first factor in the min cannot be made arbitrarily large, and the decay rate may be smaller than the one for the full state observer (see Theorem 3.10).

Thus we see that in both the cases of either velocity or density observations, the full state observers previously presented perform better than simple nudging, even with an optimal choice of the nudging convolution kernel.

4. Additional study of the observer in dimension 1. In this section, we study the same observer as in the above discussion, but in one dimension. There are a few simplification which we point out below. We extend the study of the above observer to two special cases in one dimension. In subsection 4.2, we discuss the case when the equation contains an unknown forcing term while in subsection 4.3, we consider the case when the observations are over a subdomain $[0, L]$ with $L < 1$.

4.1. Remarks about decay rates in one dimension. Essentially all the results in the previous section are also applicable in one dimension with the only difference being the absence of certain eigenvalues, as we discuss in this subsection. Noting that $\mu\Delta u + (\lambda+\mu)\nabla(\nabla\cdot u) = \nu u_{xx}$ in one dimension with $\nu = 2\mu+\lambda$, we can simplify (3.1) to the following:

$$r_t + \rho_0 v_x = -\rho_0 \varphi_\rho * v_x\,, \quad \rho_0 v_t = \nu v_{xx} - \gamma\rho_0^{\gamma-1} r_x - \rho_0 \varphi_u * v\,, \tag{4.1}$$

whereas (3.4) simplifies to

$$\rho_0 v_{tt} = \nu v_{txx} + \gamma\rho_0^{\gamma} v_{xx} + \gamma\rho_0^{\gamma}\varphi_\rho * v_{xx} - \rho_0\varphi_u * v_t\,. \tag{4.2}$$

From this, we can see that the matrices M_k and N_k from (3.10) and (3.13), respectively, will remain the same, noting that $k\otimes k = |k|^2 = k^2$. These 2×2 matrices will not have eigenvalues λ_{0k} or λ_{dk} but only two eigenvalues $\lambda_{\pm k}$ as given in (3.15) with the same eigenvectors as given before.

Hence the main result in Theorem 3.6 also applies in one dimension, with the following modification to the choice of φ_{uk}:

$$\varphi_{uk} = \max\left\{0; 2d - (c_1+c_2)k^2)\right\} = \max\left\{0; 2d - \frac{\nu 4\pi^2 k^2}{\rho_0}\right\},$$

and the same choice of $\varphi_{\rho k}$ as in (3.23):

$$\varphi_{\rho k} = \max\left\{0; \frac{\left((c_1+c_2)|k|^2\right)}{4c_5|k|^2} - 1\right\} = \max\left\{0; \frac{\left(\frac{\nu 4\pi^2 k^2}{\rho_0} + \varphi_{uk}\right)^2}{16\pi^2\gamma\rho_0^{\gamma-1}k^2} - 1\right\}.$$

Further, in the case of density observations, the result in Theorem 3.10 is even stronger, in the sense that with the choice of $\psi_{\rho k}$ and ψ_{uk} of (3.34)–(3.35), the decay rate is at least d, since there is no nontrivial incompressible flow field in one dimension.

4.2. Unknown forcing term. We now consider observers for the linearized 1D equations with a forcing term in the velocity equation. For simplicity, we also assume that $\rho_0 = 1$ and, as earlier, without loss of generality, we assume $u_0 = 0$:

$$\rho_t + u_x = 0\,, \quad u_t = \nu u_{xx} - \gamma\rho_x - f(x,t)\,. \tag{4.3}$$

If this forcing term $f(t,x)$ is known, then we also add it to the velocity equation of the observer (2.8). Then, by considering the difference between the observer and original equations, the forcing term disappears and we are still considering (4.1) for the error.

So we now assume that the forcing term is unknown. In this case, we cannot add it inside the observer equation. So the observer equation remains unchanged, and then, the difference between the reference velocity and the observer velocity satisfies (4.2) with a forcing term:

$$v_{tt} = \nu v_{txx} + \gamma v_{xx} + \gamma\varphi_\rho * v_{xx} - \varphi_u * v_t + f_t\,. \tag{4.4}$$

We now adapt the spectral analysis. We assume that the mean of f is 0 (no bias in the forcing), and then the Fourier decomposition of f is

$$f(t,x) = \sum_{k\neq 0} f_k(t) e^{i2k\pi x}.$$

Then from (3.12), we obtain the following new equation for the kth mode of the error:

$$a_k''(t) + \left(\varphi_{uk} + 4\nu k^2\pi^2\right)\, a_k'(t) + 4k^2\pi^2\gamma(1+\varphi_{\rho k})\, a_k(t) = f_k'(t). \tag{4.5}$$

We just need to find a particular solution to this equation, and add it to the general solution that we found in section 3.3.

We consider a very simple case (for reasons of clarity and for a better understanding of the phenomenon), where the time dependence of the forcing is a sine (or cosine) function:

$$f_k(t) = c_k \sin(2\omega_k \pi t), \tag{4.6}$$

where ω_k is the frequency of the forcing oscillation of mode k. Defining $\alpha_k = \varphi_{uk} + 4\nu k^2\pi^2$ and $\beta_k = 4k^2\pi^2\gamma(1+\varphi_{\rho k})$, (4.5) becomes

$$a_k''(t) + \alpha_k a_k'(t) + \beta_k a_k(t) = 2c_k\omega_k\pi\cos(2\omega_k\pi t). \tag{4.7}$$

A particular solution is then given by

$$a_k(t) = A_k\cos(2\omega_k\pi t) + B_k\sin(2\omega_k\pi t). \tag{4.8}$$

The constants A_k and B_k are a solution of the following linear system:

$$\begin{aligned} A_k\left(\beta_k - 4\omega_k^2\pi^2\right) + B_k(2\omega_k\pi\alpha_k) &= 2c_k\omega_k\pi, \\ A_k(-2\omega_k\pi\alpha_k) + B_k\left(\beta_k - 4\omega_k^2\pi^2\right) &= 0. \end{aligned}$$

Then, we get

$$A_k = 2c_k\omega_k\pi\frac{\beta_k - 4\omega_k^2\pi^2}{(\beta_k - 4\omega_k^2\pi^2)^2 + (2\omega_k\pi\alpha_k)^2}, \tag{4.9}$$

$$B_k = 2c_k\omega_k\pi\frac{2\omega_k\pi\alpha_k}{(\beta_k - 4\omega_k^2\pi^2)^2 + (2\omega_k\pi\alpha_k)^2}. \tag{4.10}$$

The amplitude of the particular solution is then given by

$$D_k = \sqrt{A_k^2 + B_k^2} = \frac{2c_k\omega_k\pi}{\sqrt{(\beta_k - 4\omega_k^2\pi^2)^2 + (2\omega_k\pi\alpha_k)^2}}. \tag{4.11}$$

Increasing $\varphi_{\rho k}$ or φ_{uk} (or both) will make β_k or α_k (or both) increase, and then D_k will decrease. This means that we can make D_k become as small as we want and the observer will converge towards the true state. But of course, the numerical performance of the observer is severely degraded in comparison with previous cases, as it is usually not possible to consider extremely high values of feedback coefficients from a numerical point of view.

Concerning the density, adapting the previous calculations on the decrease of ρ (knowing the decrease of u), we get the following amplitude of the particular solution:

$$E_k = \frac{k}{\omega_k}(1+\varphi_{\rho k})\, D_k, \tag{4.12}$$

which means that one can adapt the limit amplitude of ρ by changing the values of $\varphi_{\rho k}$. Theoretically, choosing $\varphi_{\rho k} = -1$ has the effect of completely removing the influence of the forcing term on the density but, of course, it is not numerically stable or physically consistent to consider negative feedback coefficients.

4.3. Heuristic in the case of observations over a part of the domain. In the case of observations over only a part of the domain, we define the observation domain $\Omega = [0, L]$ with $L < 1$. In this case, in order to proceed with Fourier analysis, we will need to find the Fourier transform of $v\mathbb{1}_\Omega$ because the feedback terms $\varphi * v$ will be replaced with $\varphi * (v\mathbb{1}_\Omega)$. The Fourier series for $\mathbb{1}_\Omega$ is

$$\mathbb{1}_\Omega = L + \sum_{k=1}^{\infty} \left[\frac{\sin 2\pi kL}{k} \sin 2\pi kx + \frac{1 - \cos 2\pi kL}{k} \cos 2\pi kx \right] . \tag{4.13}$$

Thus we see that the Fourier series of $v\mathbb{1}_\Omega$ will have Fourier components for all k even in the case when v has just a single Fourier mode.

Such coupling of Fourier modes will numerically slightly degrade the performance of the observer, as at any time, some energy will be transferred between different Fourier modes, as in the full nonlinear model.

If we rewrite (4.2) (for simplicity with $\rho_0 = 1$), we get

$$v_{tt} = \nu v_{txx} + \gamma v_{xx} + \gamma \varphi_\rho * (v_{xx}\mathbb{1}_\Omega) - \varphi_u * (v_t \mathbb{1}_\Omega) . \tag{4.14}$$

Then, for reasons of simplicity, assuming v only has one single Fourier mode k, (4.5) rewrites as

$$a_k''(t) + \left(L\varphi_{uk} + 4\nu k^2\pi^2\right) a_k'(t) + 4k^2\pi^2\gamma(1 + L\varphi_{\rho k})\, a_k(t) = 0. \tag{4.15}$$

Indeed, only the zeroth order term (L, from (4.13)) in the Fourier decomposition of $\mathbb{1}_\Omega$ will be kept through the convolution with v (or one of its derivatives). So, the decay rate becomes

$$\frac{\varphi_{uk} L + 4\nu k^2\pi^2}{2}. \tag{4.16}$$

Of course, this is an approximation, as even if v only has a single Fourier mode at time $t = 0$, the convolution with a characteristic function leads to mode mixing, as in a nonlinear situation. But we assume here that most of the energy is along mode k (if only this mode is present at the initial time), which will be confirmed by numerical experiments in the next section.

5. Numerical experiments on the 1D compressible Navier–Stokes observer. In this section, we report some of the numerical investigations in one dimension that illustrate the linear theory we discussed above. We also present results of using the same observer as in the linear case for two additional scenarios, namely, (i) the observer when the velocity is observed only over a subinterval of the domain in section 5.4, and (ii) in section 5.5, observer for the fully nonlinear equations.

5.1. Numerical configuration. The space domain is $[0, 1]$ and we still assume periodic boundary conditions. The discretization involves 10^2 grid points, with a step $\Delta x = 10^{-2}$. We consider a time step $\Delta t = 10^{-3}$. We also experimented with increasing the spatial resolution (and, correspondingly, decreasing the time step), but the results are almost identical and not presented here. The adiabatic exponent is set to $\gamma = 1.4$, and the diffusion is set to $\nu = 5 \cdot 10^{-2}$ (except in section 5.5). The numerical code uses a conservation form of the compressible Navier–Stokes system, with ρ and ρu as variables. A finite volume scheme is used, in which the inviscid flux is computed using an approximate Riemann solver (e.g., VFRoe scheme). The time

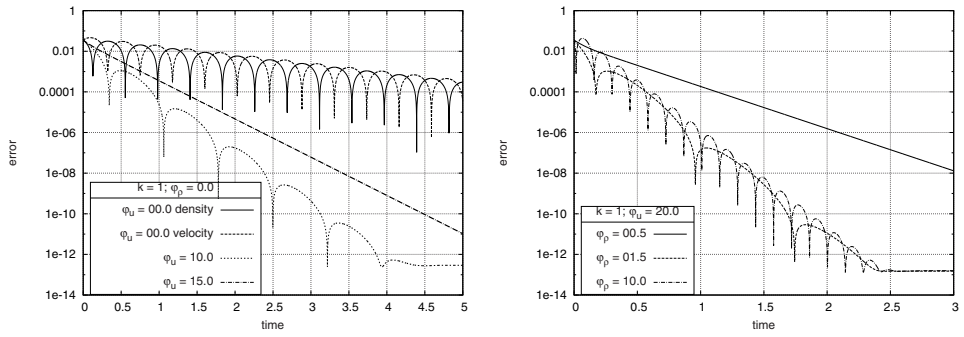

FIG. 1. *The L^2 norm of the difference between the observer $(\hat{\rho}, \hat{u})$ and the solution (ρ, u) versus time. Solid and dotted lines are the errors in ρ and u, respectively. The left panel is for fixed $\varphi_\rho = 0$ with varying φ_u while the right panel is for fixed $\varphi_u = 20$ with varying φ_ρ.*

integration scheme is a third order explicit Runge–Kutta scheme, where the time step is chosen based on a CFL condition.

In order to reproduce a quasi-linear situation, we consider the true (observed) solution $\rho(t,x) = 1$ and $u(t,x) = 0$ while the initial conditions for the observer are set to

$$\hat{\rho}_I(x) = 1 + 5 \cdot 10^{-2} \sin(2\pi k x), \quad \hat{u}_I(x) = 5 \cdot 10^{-2} \sin(2\pi k x), \tag{5.1}$$

so that the mean values of $\hat{\rho}$ and $\hat{u}$ are $\rho_I = 1$ and $u_I = 0$, respectively, and where k is a given mode, usually the first one ($k = 1$, unless differently specified).

We first look at the solution without any feedback term; see (2.8) with $\varphi_u = \varphi_\rho = 0$. Figure 1 (solid and dashed curves, left panel) shows the evolution (in log scale) of the L^2 norm of the difference between the observer $(\hat{\rho}, \hat{u})$ and the solution (ρ, u). As there is no feedback, all the Fourier coefficients $\varphi_{\rho k}$ and φ_{uk} are equal to 0, and then from (3.18), the discriminant is $\Delta \simeq -217.2$, and the theoretical decay rate (only due to diffusion) is given by (3.15): $d_{th} = 0.987$. Also the oscillation period can be computed from (3.15) and (3.18): $\omega_{th} = \frac{4\pi}{\sqrt{-\Delta}} \simeq 0.85$.

Numerically, the slope of the solid curve in the left panel of Figure 1 gives a numerical decay rate $d_{\text{num}} = 0.980$. Note that the figures show the errors to base 10, hence the slope of the semilog plot is $d_{\text{num}}/\log(10) = 0.426$. The numerical oscillation period is approximately $\omega_{\text{num}} = 0.852$. Note that one period corresponds to two oscillations on the figure for the norm of the cosine. This excellent agreement between theoretical and numerical values can be reproduced for other modes and other values of the parameters.

5.2. Simple nudging observer. We now consider the nudging framework (see section 3.6 and (3.37)), and we, hence, suppose that there is some feedback only in the velocity equation. We then first let $\varphi_\rho = 0$, and only modify the values of φ_u. This simulates the nudging, or asymptotic observer: as only the velocity is measured, only the velocity is corrected in the observer system. Table 1 shows the theoretical and numerical decay rates and oscillation periods for several values of φ_{u1}.

The first remark is that the numerical results perfectly match the theoretical results, except for the particular value of $\varphi_{u1} = 12.895$. In this case, the numerical decay rate is slightly smaller than the theoretical one. Also, no oscillations can be seen on the results, which is reasonably in agreement with a theoretical period of 81 which will be impossible to see with a final time of $T = 5$.

TABLE 1

Theoretical and numerical decay rates and oscillation periods for several values of φ_u ($k = 1$, $\varphi_\rho = 0$). The values in parenthesis give the numerical decay rates in base-10, in order to compare with slopes of lines in Figure 1.

φ_{u1}	Theoretical decay rate	Numerical decay rate	Theoretical oscillation period	Numerical oscillation period
0	0.987	0.980(0.426)	0.85	0.86
0.1	1.037	1.032	0.85	0.85
0.5	1.237	1.237	0.86	0.85
1	1.487	1.486	0.86	0.87
5	3.487	3.485	0.97	0.98
10	5.987	6.012(2.61)	1.42	1.38
12.895	7.434	6.590	81.0	–
15	4.393	4.364(1.895)	–	–
20	2.897	2.861	–	–

TABLE 2

Theoretical and numerical decay rates and oscillation periods for several values of φ_ρ with fixed $\varphi_u = 20$ for the $k = 1$ mode. (The values in parenthesis are again decay rates in base 10 for comparison with Figure 1.)

$\varphi_{\rho 1}$	Theoretical decay rate	Numerical decay rate	Theoretical oscillation period	Numerical oscillation period
0	2.897	2.861	–	–
0.5	4.838	4.790(2.080)	–	–
1.184	10.94	9.74		
1.5	10.98	11.03(4.791)	1.50	1.57
5	10.99	11.03	0.43	0.43
10	10.99	11.06(4.802)	0.28	0.28

As φ_{u1} increases, the decay rate increases, until φ_{u1} reaches $4\pi\sqrt{\gamma} - 4\nu\pi^2 \simeq 12.895$ (see remark in section 3.6), for which the discriminant is equal to 0, and then positive for increasing φ_{u1}. The corresponding optimal decay rate is $d_{th} = 2\pi\sqrt{\gamma} \simeq 7.434$ (see section 3.6). We can see that the decay rate then decreases, as the discriminant takes larger positive values, so that one of the two eigenvalues gets closer to 0.

One can see on Figure 1 (left panel, dotted and dash-dotted curves) that the error decreases much more strongly than in the case of no feedback (Figure 1, left panel, solid curve). We can also see that with increasing φ_u, the period of oscillations increases and eventually there are no oscillations (discriminant is positive). It confirms that the decay rate decreases if φ_{u1} is increased too much.

Similar results have been observed for other values of the diffusion ν, and for other modes k, and in each case, these numerical results match well with the theoretical predictions.

5.3. Results on the full state observer. We now use the full state observer, with an additional feedback term in the density equation (see (3.5)). We refer here to theoretical results from sections 3.3 and 3.4. We first set $\varphi_{u1} = 20$, for which the discriminant is positive, the largest eigenvalue gets closer to 0, and then the decay rate becomes nonoptimal.

Table 2 shows the theoretical and numerical decay rates (and oscillation periods) for several values of $\varphi_{\rho 1}$. As the discriminant is positive when $\varphi_{u1} = 20$ and $\varphi_{\rho 1} = 0$, (3.23) gives the theoretical value for which the discriminant comes back to negative values: $\varphi_{\rho 1} = \frac{(\varphi_{u1} + 4\nu\pi^2)^2}{16\gamma\pi^2} - 1 \simeq 1.184$.

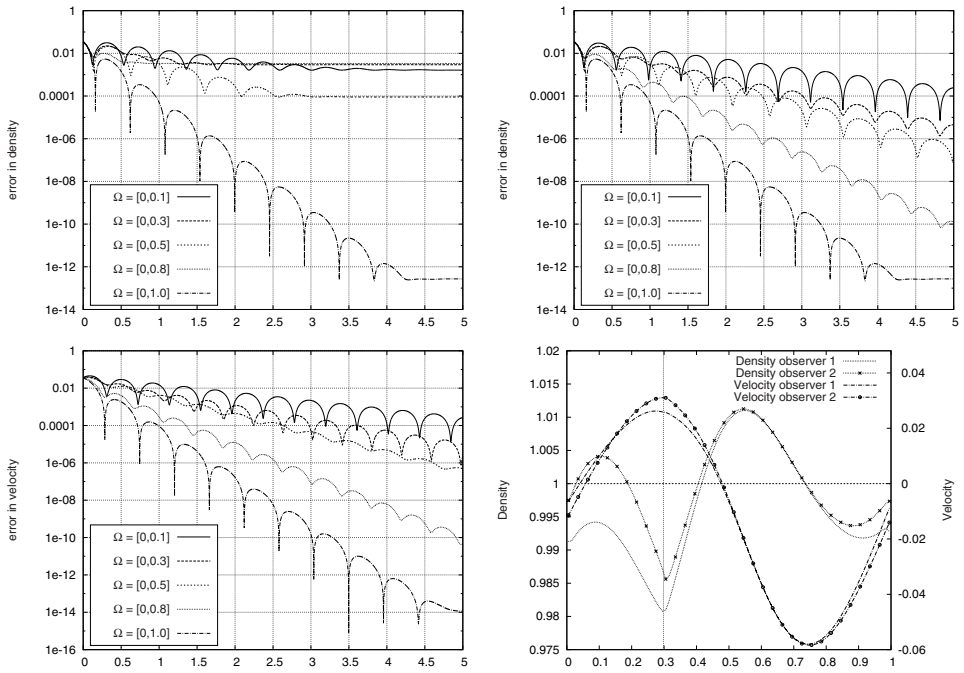

FIG. 2. *L^2 norm of the difference between the observer $\hat{\rho}, \hat{u}$ and the solution ρ, u, in the case of observations over the subinterval $[0, L]$ for $L = 0.1, 0.3, 0.5, 0.8, 1$, all of them with the strength of the feedback terms being $\varphi_\rho = 0.5$ and $\varphi_u = 10$. Left panels are for feedback from (2.5) while the top right panel is for feedback from (5.2). The error in velocity for the feedback from (5.2) is almost identical to the bottom left panel and hence not shown. The bottom right panel shows the observer solutions at time $t = 0.16$. Note that "observer 1" refers to (2.5) while "observer 2" refers to (5.2).*

We observe numerically that the decay rate is very similar to the theoretical rate, and we clearly observe the transition from positive to negative discriminant with the stabilization of the decay rate, and the apparition of oscillations. Increasing $\varphi_{\rho 1}$ to a much larger value than the optimum given by (3.23) is not necessary, as the decay rate does not increase, and the period of oscillations increases quite quickly. This is clearly seen from the plots in the right panel of Figure 1.

As we have seen, by adding the derivative of the velocity as a feedback to the density equation, we were able to significantly increase the decay rate of the error, in comparison with only a feedback in the velocity equation.

5.4. Observers with observations over a part of the domain. In this section we present the numerical results of the full state observer (see (2.5)), but with observations over only a part of the domain. The left panels of Figure 2 show the decay rate of the L^2 error between the observer $(\hat{\rho}, \hat{u})$ and the actual solution (ρ, u).

We see that, as expected from section 4.3, the rate of decay is smaller for smaller observational intervals. We also see that the error in velocity decreases linearly (with oscillations) whereas the error in density saturates at a fairly high but constant value. This is because the solution of the observer equation converges to a solution with $\hat{u} = 0$ but with $\hat{\rho} = \rho_n$, where $\rho_n \neq \rho_I$, i.e., the observer density is shifted by an amount which compensates for the initial discrepancy between the mean of $\hat{\rho}$ and the mean of ρ. This is not surprising since the original equations themselves are invariant under the constant shift in density.

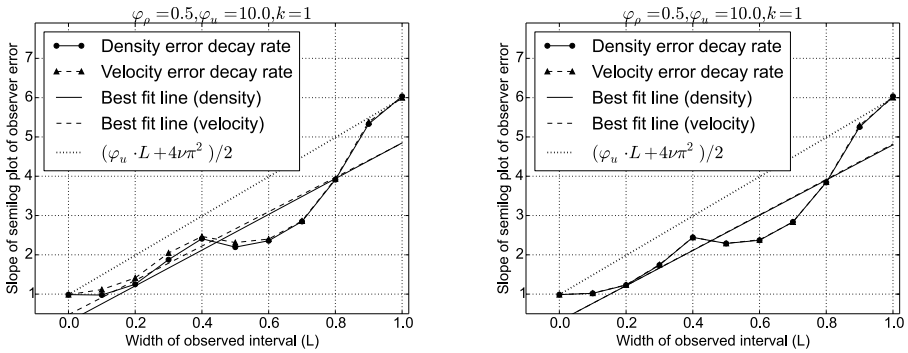

FIG. 3. *The decay rates for the velocity and the density, as a function of the length of the observation interval (quasi-linear case in the left panel and fully nonlinear case in the right panel). Note that the slope of the best fit line* ≈ 4.5 *whereas the slope of the best fit line by taking only the points for* $L = 0.1, 0.2, 0.3, 0.4, 0.9, 1.0$ *is* ≈ 5.7.

In order to overcome this problem in the case of observations over a partial domain, we propose the following modification of the feedback terms in (2.5):

$$F_\rho(\hat{\rho}, \hat{u}, u) = \varphi_\rho * D_\rho \left[\mathbb{1}_\Omega (u - \hat{u}) - \langle u - \hat{u} \rangle \right], \tag{5.2}$$

where $\langle f \rangle$ indicates average of f over the interval $[0, L]$. This ensures that the average of the feedback term is zero and hence the equilibrium solution of this equation also has mean zero. Note that in the case of $L = 1$, i.e., the case of full observations, this average is just zero and the feedback in (5.2) is identical to that in (2.5). The errors obtained by using this new observer are shown in the right upper panel of Figure 2. We clearly see that the observer $\hat{\rho}$ now approaches the solution ρ and the error decreases as expected.

In order to clearly see the effect of the observer, the lower right panel of Figure 2 shows the actual observer solutions for the case when $\Omega = [0, 0.3]$. They clearly show the effect of incorporating the observations, and also the difference between the observer with the incorrect mean and the one with correct mean. The effect is of course more pronounced on the density than on the velocity.

In this case the discriminant of the decay rate is clearly negative (as evidenced by oscillations in the plot for errors) but we can calculate the decay rate. Figure 3 shows the decay rate of the observer as a function of the length of the interval over which the velocity is observed, for the case when $\varphi_\rho = 0.5$, $\varphi_u = 10$ for the $k = 1$ mode. We notice that this is pretty close to a straight line and the best fit line is given as follows:

$$D = 4.99L + 0.24\,. \tag{5.3}$$

Comparing this with the rate given in (4.16), we see that the last equality is a reasonable approximation. Thus even though we cannot calculate the exact decay rate (see section 4.3), a reasonable estimate can be obtained by using formula (4.16):

$$D \approx \frac{\varphi_u L + 4\nu\pi^2 k^2}{2} = 5L + 0.987 \tag{5.4}$$

in experiments corresponding to Figure 3 ($\varphi_u = 10$).

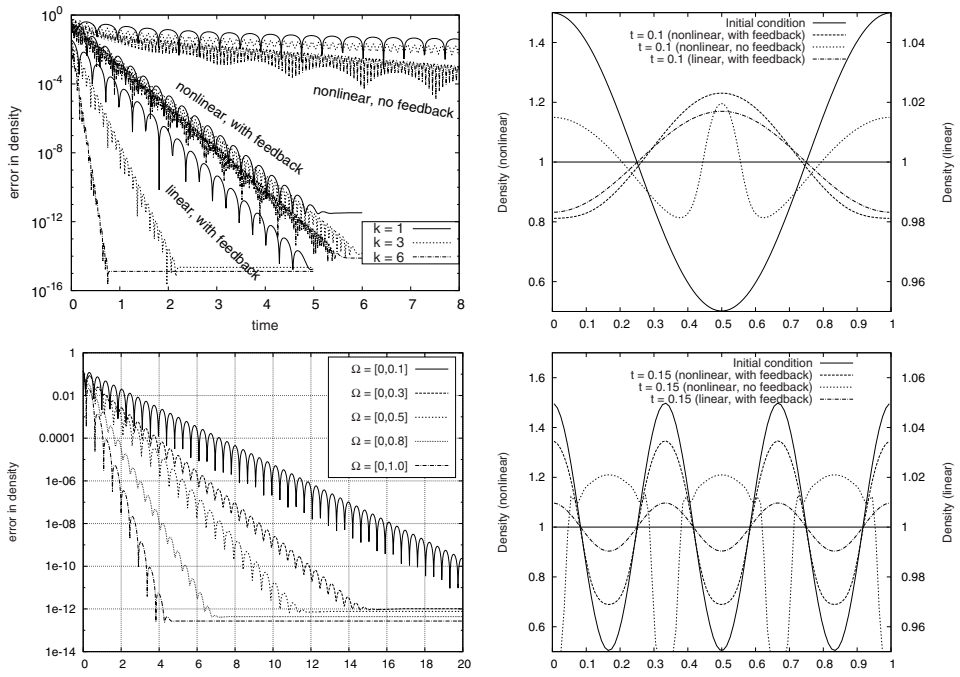

FIG. 4. *The decay rates of the nonlinear observer compared with that of the linear observer (top left). The actual observer solutions are also shown ($k = 1$ in the top right, $k = 3$ in the bottom right). The decay rates for the nonlinear observer with observations over a partial domain is in the bottom left.*

This figure shows that the global slope of the numerical decay rates versus the length of the observation interval is close to $\frac{\varphi_u}{2} = 5$. There is also a good agreement between numerical decay rates and the approximated theoretical ones (see (4.16)) when L is either small (almost no observations) or large (almost all the domain is observed), while the numerical decay rates are degraded when only half the domain is observed. When $L \approx 0.5$, previous spectral studies show that mixing of Fourier modes has a higher effect than when $L \approx 0$ or 1. Convolution with the characteristic function leads to nonnegligible transfers of energy from mode k to other modes, and then to a smaller decay rate.

But Figure 3 also shows that even with a small observed subdomain, our observer is still very efficient and we can still control the decay rate by increasing φ_u. We note that we have not considered the problem of placement of the observations, which is certainly important and has a huge influence on the decay rate [29, 19].

5.5. Observer for nonlinear Navier–Stokes system. In this section, we will report the numerical results of using the full state observer for the nonlinear system of equations, i.e., from (2.3), with the feedback terms as in (2.5), in a 1D system. Note that we do not have theoretical estimates of the decay rates towards the equilibrium solution. The aim of this section is to understand the efficiency of the above nonlinear observer.

First, we consider observations of the equilibrium solution, so that we are essentially studying the decay of the observer towards the equilibrium. The left panel of Figure 4 shows the decay rates of the observer solution with the following two initial con-

ditions, with the feedback term set to zero, and for the case with $(\varphi_\rho, \varphi_u) = (0.2, 10)$:

$$\hat{\rho}_I(x) = 1 + 5 \cdot 10^{-1} \sin(2\pi k x), \quad \hat{u}_I(x) = 5 \cdot 10^{-1} \sin(2\pi k x).$$

Note that the perturbation strength is 10 times larger than the "quasi-linear" case with the perturbation in (5.1). We consider two cases, $k = 1$ and $k = 3$. The cases with other values of $k > 1$ show a very similar behavior to the case $k = 3$ and hence are not shown here explicitly. For reference, we have also plotted the decay rates of the linear case as well.

The right panel of that figure shows the actual observer solutions for the $k = 1$ case. Note the different scales for the nonlinear (left axis) and linear (right axis) regimes. We clearly see that with a perturbation strength of $5 \cdot 10^{-1}$, even though the initial condition only has the $k = 1$ mode present, at time $t = 0.1$, higher modes are excited (dotted line, with no feedback). When the observer feedback is added, the solution very quickly decays before higher modes are excited, bringing the perturbation to the level where the linear theory is a good approximation and thus the decay rate is identical to that of the linear case of perturbation strength $5 \cdot 10^{-2}$.

The case for $k = 3$ (and indeed all higher modes with $k > 1$) is quite interesting. In this case, the initial condition of $k = 3$ excites the $k = 1$ mode. Thus even when the observer feedback is added, the decay rate is not the same as the linear $k = 3$ decay rate but rather it is closer to the linear $k = 1$ rate. The same behavior is seen for other modes with $k > 1$. Figure 4 shows example of this decay for $k = 3$ and $k = 6$, along with the actual observers. It is quite clear that in the quasi-linear case, modes other than the one contained in the initial condition are not excited while in the nonlinear case, they are quite clearly excited.

Finally, we also performed numerical experiments, still with the full state observer on the nonlinear system, but now with partial observations over various domain sizes, as discussed in section 4.3. Quite surprisingly, the behavior in the nonlinear case is very similar to the linear case: the decay rate is close to being linear in the size of the domain; see the right panel of Figure 3 and the bottom left panel of Figure 4.

6. Conclusion. In this paper, we were interested in observer design for viscous compressible Navier–Stokes equations. Thanks to intrinsic properties of the system (symmetries), we were able to design observers in order to reconstruct the full solution (both velocity and density) when only one variable (either velocity or density) is observed, even partially.

A spectral study showed that for a tangent linear system (linearized around the equilibrium state of constant velocity and density), we can prove the convergence of the observer towards the solution, and we can control the decay rate of the error, with explicit formulas for the feedback coefficients as functions of the desired decay rate.

Numerical experiments in one dimension are in perfect agreement with theory in the linearized situation: we can obtain any decay rate by increasing the observer coefficients. Numerical experiments also show that our observer is still very efficient in the case of observations over a partial domain, and also in the full nonlinear case.

The application of this kind of observer in other specific cases such as full primitive equations of the ocean or the atmosphere, will be a natural extension of this work. Observers for fluid equations coupled to other quantities such as temperature or salinity with observations of these fields instead of velocity observations will also be an interesting extension that will be of great interest in practice since these types of measurements are more common than measurements of the velocity field. It will also

be quite challenging and interesting for practical applications to consider observers in the case when observations are available discretely in time and/or in space.

Acknowledgment. The authors would like to thank both the anonymous referees for useful remarks which led to this improved revised version.

REFERENCES

[1] A. Farhat, M.S. Jolly, and E.S. Titi, *Continuous data assimilation for the* 2*d Bénard convection through velocity measurements alone*, Phys. D, 303 (2015), pp. 59–66.

[2] D.A.F. Albanez, H.J. Nussenzveig Lopes, and E.S. Titi, *Continuous data assimilation for the three-dimensional Navier–Stokes-α model*, Asymptot. Anal., 97 (2016), pp. 139–164.

[3] D. Auroux and S. Bonnabel, *Symmetry-based observers for some water-tank problems*, IEEE Trans. Automat. Control, 56 (2011), pp. 1046–1058.

[4] A. Azouani, E. Olson, and E.S. Titi, *Continuous data assimilation using general interpolant observables*, J. Nonlinear Sci., 24 (2014), pp. 277–304.

[5] Andrew F. Bennett, *Inverse Modeling of the Ocean and Atmosphere*, Cambridge University Press, Cambridge, 2002.

[6] A. Bensoussan, G. Da Prato, M.C. Delfour, and S.K. Mitter, *Representation and Control of Infinite Dimensional Systems*, Birkhäuser, Basel, Boston, 2007.

[7] H. Bessaih, E. Olson, and E.S. Titi, *Continuous Assimilation of Data with Stochastic Noise*, Nonlinearity, 28 (2015), pp. 729–754.

[8] D. Bloemker, K.J.H. Law, A.M. Stuart, and K. Zygalalkis, *Accuracy and stability of the continuous-time* 3*dvar filter for the Navier-Stokes equation*, Nonlinearity, 26 (2013), pp. 2193–2219.

[9] S. Bonnabel, P. Martin, and P. Rouchon, *Symmetry-preserving observers*, IEEE Trans. Automat. Control, 53 (2008), pp. 2514–2526.

[10] S. Bonnabel, P. Martin, and P. Rouchon, *Non-linear symmetry-preserving observers on Lie groups*, IEEE Trans. Automat. Control, 54 (2009), pp. 1709–1713.

[11] S. Chowdhury, D. Maity, M. Ramaswamy, and J-P. Raymond, *Local stabilization of the compressible Navier-Stokes system, around null velocity, in one dimension*, J. Differential Equations, 259 (2015), pp. 371–407.

[12] J. Deguenon, G. Sallet, and C. Z. Xu., *A Kalman observer for infinite dimensional skew-symmetric systems with applications to an elastic beam*, in 2nd International Symposium on Communications, Control, Signal Processing, SuviSoft Oy, Tampere, Finland, 2006.

[13] R. Droghei, B. Buongiorno Nardelli, and R. Santoleri, *Combining in situ and satellite observations to retrieve salinity and density at the ocean surface*, J. Atmos. Oceanic Tech., 33 (2016), pp. 1211–1223.

[14] S. Ervedoza, O. Glass, S. Guerrero, and J.-P. Puel, *Local exact controllability for the one-dimensional compressible Navier-Stokes equation*, Arch. Ration. Mech. Anal., 206 (2012), pp. 189–238.

[15] G. A. Gottwald, *Controlling balance in an ensemble Kalman filter*, Nonlinear Process. Geophys., 21 (2014), pp. 417–426.

[16] B. Z. Guo and Z. C. Shao, *Stabilization of an abstract second order system with application to wave equations under non-collocated control and observations*, Systems Control Lett., 58 (2009), pp. 334–341.

[17] B.-Z. Guo and C. Z. Xu., *The stabilization of a one dimensional wave equation by boundary feedback with noncollocated observation*, IEEE Trans. Automat. Control, 52 (2007), pp. 371–377.

[18] K. Hayden, E. Olson, and E.S. Titi, *Discrete data assimilation in the Lorenz and* 2*d Navier–Stokes equations*, Phys. D, 240 (2011), pp. 1416–1425.

[19] P. Hébrard and A. Henrott, *Optimal shape and position of the actuators for the stabilization of a string*, Systems Control Lett., 48 (2003), pp. 199–209.

[20] T. John, M. Guay, N. Hariharan, and S. Naranayan, *POD-based observer for estimation in Navier–Stokes flow*, Comput. Chem. Eng., 34 (2010), p. 965–975.

[21] E. Kalnay, *Atmospheric Modeling, Data Assimilation and Predictability*, Cambridge University Press, New York, 2003.

[22] D.T.B. Kelly, K.J.H. Law, and A.M. Stuart, *Well-posedness and accuracy of the ensemble Kalman filter in discrete and continuous time*, Nonlinearity, 27 (2014), pp. 2579–2603.

[23] I. Lasiecka and R. Triggiani, *Control Theory for Partial Differential Equations: Continuous and Approximation Theories*, Cambridge University Press, Cambridge, 2000.

[24] K.J.H. Law, A. Shukla, and A.M. Stuart, *Analysis of the* 3*dvar filter for the partially observed Lorenz '*63 *model*, Discrete Contin. Dyn. Syst., 34 (2014), pp. 1061–1078.
[25] J.M. Lewis, S. Lakshmivarahan, and S. Dhall, *Dynamic Data Assimilation: A Least Squares Approach*, Encyclopedia Math. Appl. 104, Cambridge University Press, Cambridge, 2006.
[26] M. Ghattassi, M. Boutayeb, and J. R. Roche, *State observer design for non linear coupled partial differential equations with application to radiative-conductive heat transfer systems*, in 53rd IEEE Conference on Decision and Control, IEEE, Piscataway, NJ, 2014, pp. 1569–1574.
[27] E. Olson and E.S. Titi, *Determining modes for continuous data assimilation in* 2*d turbulence*, J. Stat. Phys., 113 (2003), pp. 799–840.
[28] D. Park and M. Guay, *Distributed estimation for a class of nonlinear systems with application to Navier-Stokes flow estimation*, Canad. J. Chem. Eng., 93 (2015), pp. 678–688.
[29] Y. Privat, E. Trélat, and E. Zuazua, *Optimal shape and location of sensors for parabolic equations with random initial data*, Arch. Ration. Mech. Anal., 216 (2015), pp. 921–981.
[30] K. Ramdani, M. Tucsnak, and G. Weiss, *Recovering the initial state of an infinite-dimensional system using observers*, Automatica J. IFAC, 46 (2010), pp. 1616–1625.
[31] A. Smyshlyaev and M. Krstic, *Backstepping observers for a class of parabolic PDEs*, Systems Control Lett., 54 (2005), pp. 613–625.
[32] E. Sontag, *Mathematical Control Theory*, Texts Appl. Math. 6, Springer, New York, 1998.
[33] V.A. Vaigant and A. Vasil'evich Kazhikhov, *On existence of global solutions to the two-dimensional Navier-Stokes equations for a compressible viscous fluid*, Sib. Math. J., 36 (1995), pp. 1108–1141.
[34] A. Valli and W.M. Zajaczkowski, *Navier-Stokes equations for compressible fluids: Global existence and qualitative properties of the solutions in the general case*, Comm. Math. Phys., 103 (1986), pp. 259–296.
[35] R. Vazquez, E. Schuster, and M. Krstic, *A closed-form observer for the* 3*d inductionless mhd and Navier-Stokes channel flow*, in 45th IEEE Conference on Decision and Control 2006, IEEE, Piscataway, NJ, 2006, pp. 739–746.
[36] C. Z. Xu, J. Deguenon, and G. Sallet, *Infinite dimensional observers for vibrating systems*, in 45th IEEE Conference on Decision and Control, IEEE, Piscataway, NJ, 2006, pp. 3979–3983.
[37] J. Zabczyk, *Mathematical Control Theory*, Birkhäuser, Boston, 2007.